JOC The Journal of Organic Chemistry

Article

pubs.acs.org/joc

Molecular Interactions, Proton Exchange, and Photoinduced Processes Prompted by an Inclusion Process and a [2]Pseudorotaxane Formation

Amal Kumar Mandal,[†] Moorthy Suresh,[†] Manoj K. Kesharwani,[†] Monalisa Gangopadhyay,[§,∥,#] Manoj Agrawal,[†] Vinod P. Boricha,[†] Bishwajit Ganguly,*[,‡,†] and Amitava Das*[,§,∥,#]

[†]CSIR-Central Salt and Marine Chemicals Research Institute, Bhavnagar, Gujarat 364002, India

[#]Organic Chemistry Division, CSIR-National Chemical Laboratory, Dr. Homi Bhabha Rd., Pune, Maharashtra 411008, India

[‡]Academy of Scientific and Innovative Research, CSIR-Central Salt and Marine Chemicals Research Institute, Bhavnagar, Gujarat 364002, India

[§]Academy of Scientific and Innovative Research, CSIR-National Chemical Laboratory, Pune, Maharashtra 411008, India

Supporting Information

ABSTRACT: Appropriate design of the host and guest components allows formation of a novel [2]pseudorotaxane complex with an interrupted photoinduced electron transfer (PET)-coupled fluorescence resonance energy transfer (FRET) response. This is the first example of an inclusion complex with NO_6-based azacrown ether as the host unit (H). Different guest molecules (G1, G2, G3, and G4) with varying stopper size are used for the studies. Unlike G1, G2, and G3, G4 with a relatively bulkier stopper fails to form a [2]pseudorotaxane complex. Isothermal titration microcalorimetry measurements reveal a systematic increase in the association constant for H·G1, H·G2, and H·G3 with a change in the stopper size. Thermodynamic data suggest that the formation of H·G1/H·G2/H·G3 is exclusively driven by a large positive entropic gain ($T\Delta S$ = 19.69/26.80/21.81 kJ·mol^{-1}), while the enthalpy change is slightly negative for H·G1/H·G3 (−2.61/−1.97 kJ·mol^{-1}) and slightly positive for H·G2 (ΔH = 5.98 kJ·mol^{-1}). For these three inclusion complexes, an interrupted PET-coupled FRET response is observed with varying efficiency, which is attributed to the subtle differences in acidity of the NH_2^+ unit of the guest molecules and thus the proton exchange ability between the host and respective guest. This is substantiated by the results of the computational studies.

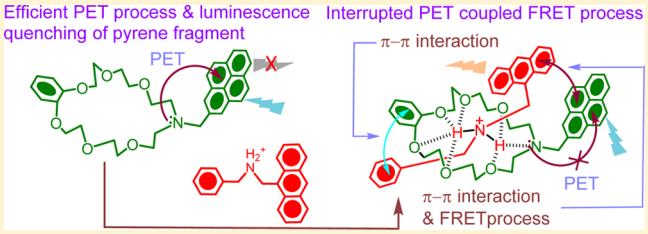

INTRODUCTION

It has long been known that crown ethers are capable of forming hydrogen-bonded adducts with organic ammonium ions.[1] Researchers have exploited this binding motif and have shown that a range of wire-type secondary ammonium ions ($R_2NH_2^+$) could be used to thread through the cavities of appropriately sized crown ether derivatives to afford interwoven complexes. This act of supramolecular recognition has very recently led to the development of new classes of molecular level devices, such as molecular switches,[2] motors,[3] rotors,[4] shuttles,[5] muscles,[6] extension cables,[7] etc. In this regard, the most studied crown ether is dibenzo-24-crown-8 (DB24C8) or its derivatives.[1e,8] Balzani et al. have also demonstrated the fluorescence resonance energy transfer (FRET)-based plug in socket function at a molecular level using inclusion complexes of a crown ether, derived from binapthol.[1c] Such an idea can be further extended to achieve a more complex system, where one can have additional control on the input signal and the consequential modified output response. To demonstrate such a process, we have utilized a supramolecular assembly where the threading phenomena result in an interrupted photo-induced electron transfer (PET) and a fluorescence on response, which in turn initiates a FRET process. Here the choice of the azacrown moiety, used as a guest, is separated from the photoactive donor unit by a $-CH_2-$ spacer, which allows the unshared pair of electrons of the tertiary N_{crown} to participate effectively in the PET process and thereby to participate in the switch-*on*/*off*-type luminescence response.[9] Though this scheme has been successfully utilized for designing sensors for metal ion recognition,[9] to date no literature report states that such a concept has been utilized for the generation of a threaded inclusion complex with an interrupted response. The appropriate choice of the donor (pyrene) and acceptor (anthracene) units, which possess the fitting spectral properties for a probable FRET process, is also crucial in the present study. To the best of our knowledge, there is no example of a relatively simple supramolecular assembly available in the literature that is capable of exhibiting a FRET process, which is

Received: April 12, 2013
Published: August 16, 2013

initiated by the luminescence on-effect due to an interrupted PET process involving the donor fluorophore.

In this paper, we report the formation of a [2]pseudorotaxane assembly from an azacrown-based host unit (H) and different secondary ammonium ion as the threaded guest (Figure 1). Importantly, interwoven complex

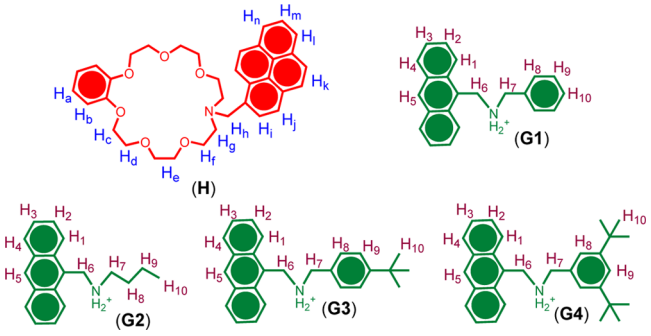

Figure 1. Molecular structure of the host and guest molecules.

formation leads to rare examples of the interrupted PET-coupled FRET process. To ensure the formation of the threaded complex involving NO_6-based azacrown ether as the host and the secondary ammonium ion as the guest component, we have also synthesized the hexafluorophosphate salt of different guest molecules (G1, G2, G3, and G4) with varying stopper size (Figure 1) and studied the complex formation process with the host molecule H using different spectroscopic techniques.

RESULTS AND DISCUSSION

Synthesis. The methodology that was adopted for the synthesis of the azacrown derivative H is shown in Figure 2. Alkylation of 1,2-dihydroxybenzene was achieved with reasonable yield by reaction with 2-[2-(2-chloroethoxy)ethoxy]-ethanol in a suspension of K_2CO_3 in DMF as the solvent. Chromatographic purification yielded the bishydroxy intermediate **1**, which was further converted to the corresponding bistosylate derivative **2**. The intermediate product **2** was allowed to react with pyren-2-ylmethanamine hydrochloride to give the desired host molecule H. The various guest molecules with different stopper sizes were synthesized by reducing the product of the Schiff base reaction between appropriate amine and aldehyde derivatives (Figure 2). These secondary amine derivatives were protonated and eventually isolated, and the desired hexafluorophosphate salts were isolated as insoluble solids by anion exchange in aqueous medium. The synthetic procedure and all relevant characterization details of these host and guest molecules are provided in the Supporting Information (SI).

Complexation of H with G1, G2, G3, and G4. The complexation of azacrown-based host H with various guest molecules (G1, G2, and G3) in $CDCl_3/CD_3CN$ (4:1, v/v) solution was first investigated in detail using ^{1}H NMR spectroscopic studies by systematically varying the concentration of the guest fragment. Let us first discuss the results of the ^{1}H NMR spectral studies involving H and G1. Partial ^{1}H NMR spectra of H, G1, and a mixture of H and G1 are shown in Figure 3.

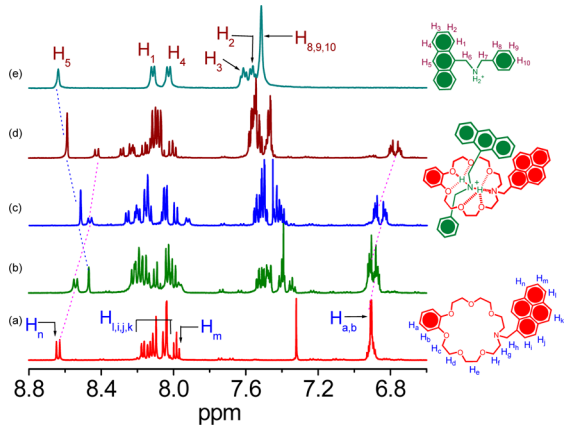

Figure 3. Partial ^{1}H NMR spectra (500 MHz, 298 K) recorded in $CDCl_3/CD_3CN$ (4:1, v/v) for (a) 7.3 mM H, (b) 7.3 mM H with 3.6 mM G1, (c) 7.3 mM H with 7.3 mM G1, (d) 7.3 mM H with 15.6 mM G1, and (e) 7.3 mM G1.

Only one set of peaks were observed in the ^{1}H NMR spectrum of the mixed solution of H and G1, which implied that the equilibrium kinetics were fast within the ^{1}H NMR time scale. Respective δ values for H_6 and H_7 of each $-CH_2-$ group of G1 were found to be shifted from 5.01 and 4.35 to 4.74 and 4.06, respectively, for 1 equiv of added G1. Signals for most of the protons, which belonged to the anthracene/phenyl ring of G1, were found to be upfield shifted relative to those signals for the free individual components (Figure 3). Thus, the observed results suggested that these aromatic protons of G1 resided under the shielding influence of the aromatic rings of the host

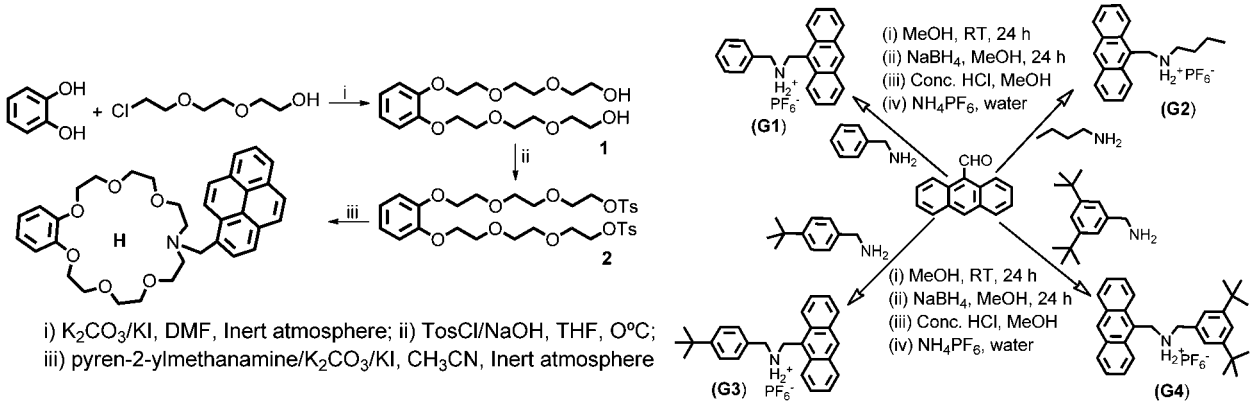

Figure 2. Methodology adopted for the synthesis of host and guest molecules.

dx.doi.org/10.1021/jo400752d | J. Org. Chem. 2013, 78, 9004−9012

molecule H during the binding process. Conversely, the nature of the shift was not uniform for the pyrene protons in host H. Appreciable upfield shifts in the signals for H_n protons ($\Delta\delta$ = −0.21 ppm) was observed, while a downfield shift was observed for H_l proton ($\Delta\delta$ = −0.13 ppm). The phenyl protons (H_a and H_b) of the host molecule H were upfield shifted ($\Delta\delta$ = −0.16 ppm) and split into two sets of signals during binding to the guest molecule G1. The difference in the shift pattern of the aromatic protons of host molecule H was mainly due to the difference in the extent of shielding of the protons due to the anisotropy of the ring current effect.

The ^{1}H NMR spectroscopic titration of H, with varying concentration of another two guest compounds, G2 and G3, also suggested the formation of host−guest complexes H·G2 and H·G3 (Figure 4 and SI Figures 2 and 3). In both cases the

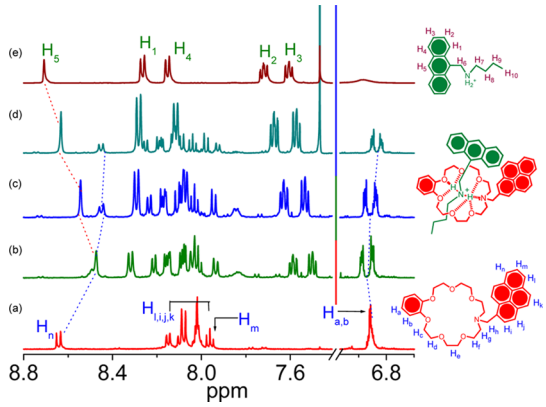

Figure 4. Partial ^{1}H NMR spectra (500 MHz, 298 K) recorded in $CDCl_3/CD_3CN$ (4:1, v/v) for (a) 6.7 mM H, (b) 6.7 mM H with 3.3 mM G2, (c) 6.7 mM H with 6.7 mM G2, (d) 6.7 mM H with 13.4 mM G2, and (e) 6.7 mM G2.

nature of the spectral shifts was found to be similar to that observed for the formation of the complex H·G1. Quite substantial complexation-induced shifts ($\Delta\delta$ = 0.47 and 0.31 ppm, respectively, for H_6 and H_7) of the methylene protons were observed in complexation of H with G2 relative to free G2. In contrast, these shifts for H_6 and H_7 for G1 in H·G1 were only 0.27 and 0.29 ppm, respectively. These significant differences in the shift values for H·G2 could be attributed to the more polarized methylene groups next to the cationic ammonium center in G2, which resulted a much stronger C−H···O hydrogen bond with the crown ether oxygen. Shifts of the ^{1}H NMR spectra for H·G3 were analogous to those observed for H·G1.

In contrast, the hexafluorophosphate salt of G4, which was substituted with relatively bulkier 3,5-di-*tert*-butyl groups, showed no apparent shift in the signals in its ^{1}H NMR spectrum when mixed with the crown ether-based host H under identical experimental conditions. Literature reports clearly suggest that the 3,5-di-*tert*-butylphenyl groups, being too big, fail to penetrate through the even bigger crown ether (DB24C8) cavity.[10] Thus, on the basis of the observations discussed above for G4, it is not unreasonable to conclude that, for the NO_6-based azacrown moiety, the pseudorotaxane formation depends on the relative size and shape of the stopper unit, and the guest molecule G4 with two bulky 3,5-di-*tert*-butyl groups failed to form an interwoven or pseudorotaxane complex with H.

The respective binding stoichiometry (1:1) for the formation of H·G1, H·G2, and H·G3 was established on the basis of the inflection point in the mole ratio plots of the ^{1}H NMR spectral studies (Figure 5). Electrospray ionization (ESI) mass spectrometry also revealed the 1:1 complex formation between H with three secondary ammonium salts (G1, G2, and G3) in the gas phase. In the case of G1, the peak was observed at *m*/*z* 864.77 for H + G1, which corroborated the formation of 1:1 complex H·G1 (SI Figure 4). The peaks at *m*/*z* 981.15 for H + G2 + PF_6^- + H^+ and *m*/*z* 1091.95 for H + G3 + PF_6^- + Na^+ also supported the formation of 1:1 complexes H·G2 and H·G3 (SI Figures 4 and 5).

Association Constant and Thermodynamics. The complexation processes and associated changes in thermodynamic parameters for the complex formation between the azacrown-based host H and different guest molecules G1−G4 were investigated in $CHCl_3/CH_3CN$ (4:1, v/v) medium by isothermal titration microcalorimetry (ITC) measurements. A good fit of the titration curve to a 1:1 binding model was also observed when analogous measurements were carried out in $CDCl_3/CH_3CN$ (4:1, v/v) solution, a conclusion that was again supported by mole ratio plot analyses in the case of the ^{1}H NMR studies (Figure 5). The corresponding titration curves for the ITC measurements and their corresponding thermodynamic parameters (inset data) are shown in Figure 6. The obtained "*N*" data, which refer to the binding sites for the complexation of three sets of complexes (*N* = 1.06 ± 0.0416 sites for G1, *N* = 0.97 ± 0.0434 sites for G2, and *N* = 0.98 ± 0.00412 sites for G3) were also consistent with a 1:1 binding model and corroborated our observations with ^{1}H NMR spectral studies.

The thermodynamic parameters obtained from the ITC titration studies are listed in Table 1. An important parameter for ITC experiments with low-affinity systems is the so-called

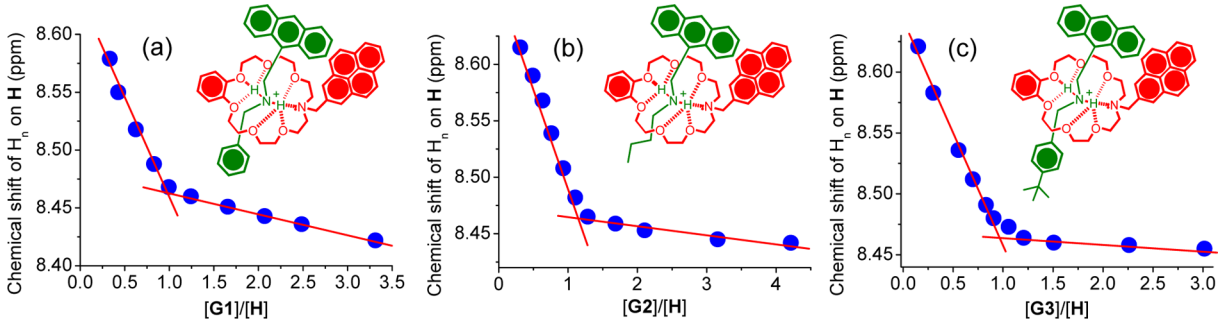

Figure 5. Mole ratio plot in $CDCl_3/CD_3CN$ (4:1, v/v) for the complexation between H and (a) G1, (b) G2, and (c) G3.

dx.doi.org/10.1021/jo400752d | J. Org. Chem. 2013, 78, 9004−9012

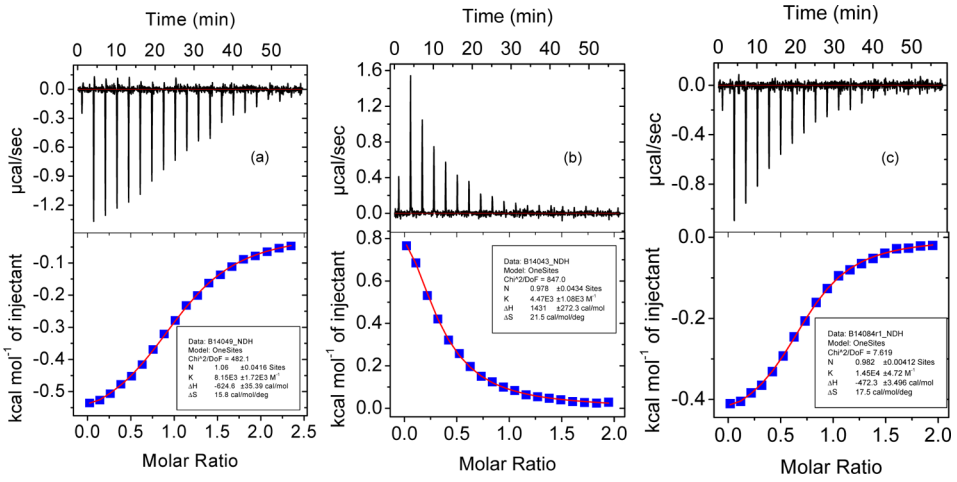

Figure 6. ITC profiles at 25 °C in $CHCl_3/CH_3CN$ (4:1, v/v) for the binding of host H (5 mM) with (a) guest G1 (50 mM), (b) guest G2 (50 mM), and (c) guest G3 (50 mM). Top: raw data for the sequential 2 μL injection of respective guests into H. Bottom: heat evolved (kcal) per mole of guest added, corrected for the heat of guest dilution, against the molar ratio of the guest to H. The data (filled circle) were fitted to a single set binding model, and the solid line represents the best fit.

Table 1. Thermodynamic Data and Association Constant Obtained from the ITC Measurements with Pseudorotaxanes Formed from Host H and Guests G1−G4[a]

host−guest complex	association constant, K_a (M^{-1})	ΔG (kJ·mol^{-1})	ΔH (kJ·mol^{-1})	$T\Delta S$ (kJ·mol^{-1})
H·G1	$(8.1 \pm 1.7) \times 10^3$	−22.30	−2.61	19.69
H·G2	$(4.47 \pm 1.0) \times 10^3$	−20.82	5.98	26.80
H·G3	$(1.45 \pm 0.4) \times 10^4$	−23.78	−1.97	21.81
H·G4	no binding was observed in the ITC experiment			

[a]ITC measurements were performed in $CHCl_3/CH_3CN$ (4:1, v/v) at 25 °C.

Wiseman "*c*" value, which is the product of the total host concentration and the binding constant K_a.[11] For $c < 10$, ITC experiments become challenging. For our studies, the respective value evaluated for *c* in each case is found to be larger than 10, and this confirms that data obtained from the ITC measurements are reliable.

As can be seen from Table 1, the association constants (K_a) for the complexation of host H with three different guest molecules (G1−G3) were obtained from the ITC titration profile. The corresponding binding constants for H·G1, H·G2, and H·G3 are $(8.1 \pm 1.7) \times 10^3$, $(4.47 \pm 1.0) \times 10^3$, and $(1.45 \pm 0.4) \times 10^4$ M^{-1}, respectively. A comparison of the observed data revealed that the value for K_a for the formation of H·G3 is 3.2 and 1.8 times higher than those for H·G1 and H·G2, respectively.

A systematic increase in the values of the association constant is observed on changing the stopper from butyl to 4-*tert*-butylphenyl in the guest molecules. This indicates that the size of the substituents on the guest molecules plays an important role in the binding affinity and also in the binding mode during the complexation process. However, no binding was observed for the complexation of H with G4 in the ITC experiment. The presence of relatively bulky stopper units such as the 3,5-di-*tert*-butylphenyl moiety prevented threading of the G4 moiety through the cavity of the NO_6-based azacrown ether unit and thus the formation of any threaded or inclusion complex. This also agrees well with the results of the ^{1}H NMR studies described earlier (vide infra).

A previous report revealed that crown ether-based pseudorotaxane complexes were mainly stabilized by hydrogen bonding (N^+−H···O and C−H···O) and $\pi-\pi$ interactions in a nonpolar solvent.[1d] The literature report also revealed that a change in guest molecule from secondary dibenzylammonium hexafluorophosphate (360 M^{-1} in acetone-d_6)[12] to the anthracenyl methyl-substituted analogue (496 M^{-1} in acetone-d_6)[13] improved the affinity of the respective guest molecule for interwoven complex formation with DB24C8. This enhanced affinity was mainly attributed to a more efficient $\pi-\pi$ interaction involving the anthracene π-system. Analogously, for the present study stronger binding of H with G1 and G3 compared to G2 was mainly due to the presence of the phenyl unit, which stabilized the adducts through an additional π-interaction. However, the higher stability of H·G3 compared to H·G1 could perhaps also reflect the presence of a bulkier 4-*tert*-butyl group, which presumably helped in forming a relatively more rigid adduct.

The obtained thermodynamic data clearly indicate that the complexation of azacrown-based host H with guests G1 and G3 in $CHCl_3/CH_3CN$ (4:1, v/v) is exclusively driven by a large positive entropic gain ($T\Delta S$ = 19.69−21.81 kJ·mol^{-1}) and is accompanied by small negative enthalpy changes ($-\Delta H$ = 2.61−1.97 kJ.mol^{-1}), as shown in Table 1. In contrast, the complexation of H with G2 is driven by a large positive entropic gain ($T\Delta S$ = 26.80 kJ·mol^{-1}) along with a small positive change in enthalpy (ΔH = 5.98 kJ·mol^{-1}).

It is generally accepted that the association process arising from conformational freedom and the desolvation effect is entropically favored ($T\Delta S > 0$).[14] It is also known that the negative enthalpy contributions ($\Delta H < 0$) arise mainly from the electrostatic, hydrogen-bonding, $\pi-\pi$, and van der Waals interactions upon complexation of the host with a guest.[14] In the present case, both the host and all guest molecules (G1, G2, and G3) have the same charge number and binding units. Thus, the size and nature of the different stopper units (e.g., phenyl for G1, butyl for G2, and 4-*tert*-butylphenyl for G3) must play a crucial role in dictating the small but realistic change in thermodynamic data. The obtained data clearly indicate that the entire complexation process is exclusively driven by a large positive entropic gain. Complexation with the guest molecule

dx.doi.org/10.1021/jo400752d | J. Org. Chem. 2013, 78, 9004−9012

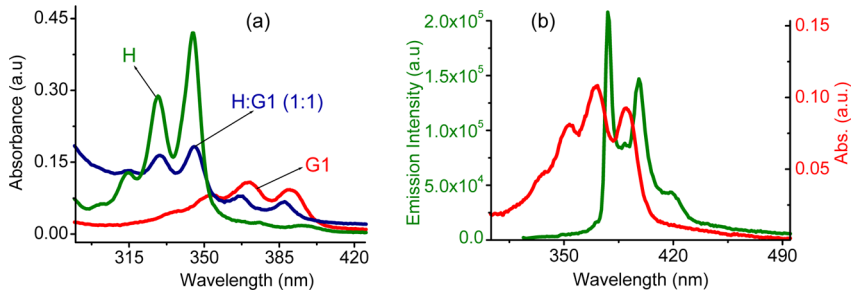

Figure 7. (a) UV–vis spectra for H ([H] = 1.11×10^{-5} M), G1 ([G1] = 3.24×10^{-6} M), and the adduct H·G1 (1:1) and (b) spectral overlap between donor (host H) emission and acceptor (guest G1) absorption in CH_2Cl_2/CH_3CN (99:1, v/v). λ_{ext} = 314 nm was used for recording the emission spectra for H.

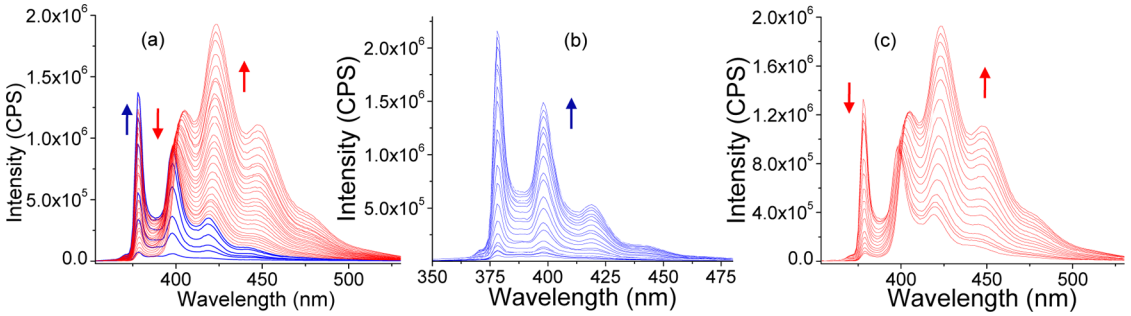

Figure 8. Fluorescence titration in CH_2Cl_2/CH_3CN (99:1, v/v) medium (λ_{ext} = 314 nm) for H ([H] = 1.12×10^{-5} M) with [G1] varying (a) from 0 to 3.90×10^{-4} M, (b) from 0 to 1.16×10^{-5} M, while pyrene-based fluorescence was enhanced until [G1] = 1.16×10^{-5} M, and (c) from 1.16×10^{-4} to 3.90×10^{-4} M, while a gradual decrease in pyrene-based emission with a concomitant increase in anthracene-based emission was observed.

G2, which has a more conformationally flexible *n*-butyl stopper unit, is driven by a comparatively larger positive entropic gain than that with G3 and G1. Enthalpy changes due to complexation are relatively small but decisive enough to reflect differences due to structural variations. The presence of a phenyl stopper in the case of G1 and G3 is mainly responsible for the negative enthalpy change during the adduct formation, which helps to stabilize adducts through H-bonding in addition to $\pi-\pi$ interaction. In the case of G2, the stability arises only from H-bonding, which is accountable for the positive enthalpy change. The more negative enthalpy change for G1 ($-\Delta H$ = 2.61 kJ·mol^{-1}), compared to that for G3 ($-\Delta H$ = 1.97 kJ·mol^{-1}), could be accounted for if one considers the more acidic nature of the hydrogen atoms of the NH_2^+ unit of G1, which helps in forming stronger H-bonds with the crown ether moiety.

Photophysical Study. The absorption spectrum recorded for azacrown-based host H was dominated by the absorption maxima at 314, 328, and 344 nm, which are characteristic for the pyrene moiety (Figure 7a). For G1, the absorption spectrum was dominated by the absorption band of the anthracene moiety with absorption maxima at 350, 370, and 390 nm. Analogous absorption spectra were also observed for G2 and G3. The host molecule H showed a very weak emission at 378 nm on excitation at any one of these three (314, 328, and 344 nm) wavelengths. The weak pyrene-based emission is explained on the basis of the PET process involving the unshared pair of electrons of the tertiary $-N_{azacrown}$ and the HOMO of the photoexcited pyrene moiety.[9] To check the complexation-induced change between H with the guest molecule G1, fluorescence spectra were recorded for a solution of H with increasing [G1] in CH_2Cl_2 using 314 nm (λ_{ext}^{pyr}) as the excitation wavelength (Figure 8). Interestingly, during the initial addition of G1 (~1 mol equiv with respect to [H]), only an enhancement in the pyrene-based emission at 378 nm was observed (Figure 8a,b). This observation tends to suggest that, during initial addition of G1, the concentration of the H-bonded adduct H·G1, involving the lone pair of electrons on N_{crown}/O_{crown} through $[N^+-H]_{G1}\cdots OH/[C-H]_{G1}\cdots OH$ interactions, increases and accounts for the interruption of the PET process. This interrupted PET process could be attributed to the observed enhancement of the pyrene-based emission.[9] On further addition of G1 ([G1]/[H] > 1) to this solution, the pyrene-based emission at 378 nm was found to decrease with a concomitant increase in the anthracene-based emission at 425 and 450 nm (Figure 8a,c).

Figure 7a clearly reveals that the anthracene moiety in G1 does not absorb at 314 nm, and thus, the observed enhancement in anthracene-based emission on excitation of the pyrene fragment at 314 nm in the hydrogen-bonded adduct H·G1 implies an efficient FRET-based process involving the donor pyrene fragment and the acceptor anthracene unit in the [2]pseudorotaxane. A possible FRET-based process is further corroborated by the fact that there exists a significant spectral overlap between the emission spectra of the donor $pyrene_H$ and the acceptor $anthracene_{G1}$ centers (Figure 7b), which thus constitute an appropriate pair for fluorescence resonance energy transfer.[15] To further support this phenomenon, we have also recorded the emission spectra of the same molar solution of G1 in the presence and absence of H at the same excitation wavelength of 314 nm. Thus, a comparison of the results of the steady-state emission studies for H·G1 with those for G1 alone strongly suggests that an efficient FRET process is operational between pyrene as the donor and anthracene acceptor units in the hydrogen-bonded adduct. The energy transfer (ET) quantum yield for the H·G1 complex was

dx.doi.org/10.1021/jo400752d | J. Org. Chem. 2013, 78, 9004–9012

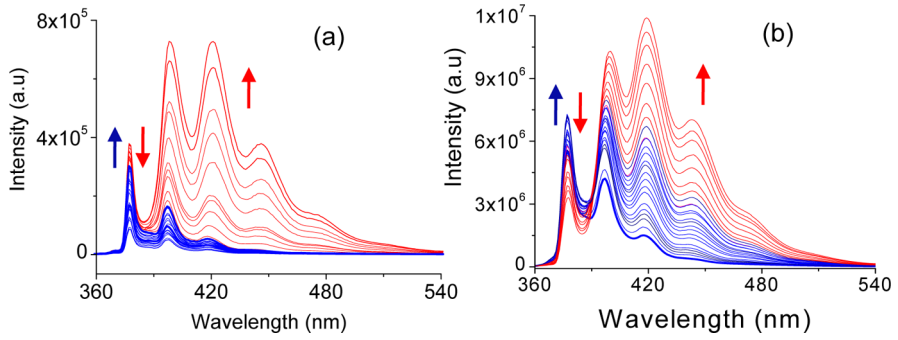

Figure 9. Fluorescence titration in CH_2Cl_2/CH_3CN (99:1, v/v) medium (λ_{ext} = 314 nm) for H ([H] = 1.54 × 10^{-6} M) with varying (a) [G2] from 0 to 5.39 × 10^{-5} M and (b) [G3] from 0 to 6.31 × 10^{-4} M.

calculated to be 22.8%.[16] The ET rate was evaluated by using a standard equation and was found to be 1.51 × 10^7 s^{-1}.[16] These data also enable us to calculate the Förster distance of 48.4 Å (R_0) by using a standard equation reported previously (SI p 9).[17]

We also recorded the emission spectra of H in the presence of three other guest molecules (G2, G3, and G4) to study the complexation process in CH_2Cl_2/CH_3CN (99:1, v/v) medium following excitation at 314 nm. The trend in the changes in the spectral pattern for H observed on formation of the complex with G2 and G3 was similar to that found for the complexation with G1 (Figure 9). During the initial stages of the addition of G2 or G3 (until [G2]/[H] or [G3]/[H] < 1 equiv) to a solution of H, the pyrene-based emission at 378 nm was found to increase due to the interruption of the PET process. However, this enhancement in emission intensity at 378 nm (3.4-fold for G2 and 1.3-fold for G3) was much lowered compared to that of the complexation with G1 (37.5-fold). This clearly revealed that the interruption of the PET process was most efficient in the case of H·G1. These observations perhaps tend to suggest that the subtle differences in the acidity of the hydrogen atoms in the $NH_2^+{}_{guest}$ moiety of the respective guest molecule must play a crucial role either in establishing an effective H-bond involving the unshared pair of electrons residing on the N-atom of the NH_H moiety (of the host component) or in a possible H^+ transfer from the NH_2^+ unit of the guest molecule to the NH_H moiety during the adduct (H·G*x*; *x* being 1 or 2 or 3) formation, as either or both of these processes in combination could be responsible for this observed pyrene-based emission enhancement. Thus, as we have assumed that the NH_2^+ units of G1 are more acidic in nature compared to those of G2 and G3, G1 shows more emission enhancement (37.5-fold) during the complexation process with H. This result was further supported by the calculated proton affinity of the N-atom of the NH_H moiety in the azacrown ether-based host molecule and the respective amine fragment ($-NH_2$) of the guest molecules through detailed DFT studies (vide infra). Conversely, no complexation-induced change in the emission spectrum of H was observed in the presence of the guest molecule G4. This further nullifies the possibility of formation of any type of adduct due to the presence of a relatively bulky stopper unit.

Computational Study. The complexation between H and guest molecule G1 was also examined using density functional theory calculations. All geometries were optimized using the B3LYP/6-31G* level of theory in the gas phase.[18] Furthermore, energy calculations have been performed in DCM medium with the B3LYP/6-31+G**//B3LYP/6-31G* level of theory using the integral equation formalism polarizable continuum model (IEF-PCM) of solvation.[19] The calculated results show that, for the interwoven complex H·G1, head to head interaction between $anthracene_{G1}$ and $pyrene_H$ was energetically preferred over the head to tail orientation by 12.5 kJ·mol^{-1} in CH_2Cl_2 medium (Figure 10). A conformation with head to head

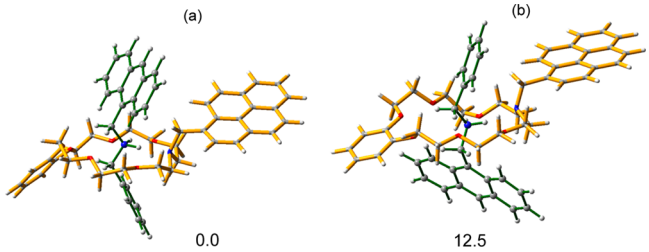

Figure 10. B3LYP/6-31+G**(DCM)//B3LYP/6-31G*-calculated relative energy (kJ·mol^{-1}) for (a) head to head and (b) head to tail alignment of an interwoven thread complex of H and G1 using the PCM (the H molecule is represented in tube form, and the G1 molecule is represented in ball and stick form).

orientation between the $anthracene_{G1}$ moiety and the $pyrene_H$ moiety could possibly be better suited for the transfer of a H^+ from $\{-(H)NHR^+\}_{G1}$ to $\{-(N)H_2\}_H$ and eventually results in a more efficient FRET process with pyrene as the donor moiety and anthracene as the acceptor moiety. Furthermore, to examine the feasibility of proton transfer from various guest molecules (G1, G2, and G3) to the host molecule H, the proton affinities of the host and respective amine of the guest molecules have been calculated using the B3LYP/6-31+G**-(DCM)//B3LYP/6-31G* level of theory (SI Figure 6). The calculated proton affinity (PA) for host molecule H in DCM medium has been found to be 1178.3 kJ·mol^{-1}, which is ∼5 kJ·mol^{-1} higher than that of the respective amine of the guest molecule G1 (PA = 1173.7 kJ·mol^{-1}) (SI Figure 6). Furthermore, the calculated proton affinity for the amine of the respective guest molecule G3 has been found to be 1176.7 kJ.mol^{-1}, which is also lower than the proton affinity of H (SI Figure 6). These results suggest that there is a possibility of more effective proton transfer from the respective NH_2^+ unit of the guest molecule to the N-atom of the NH fragment of the NO_6-based host molecule H. This also suggests that the larger difference in proton affinity values between H and G1 was mainly responsible for the large pyrene-based emission enhancement during the complexation between H and G1, compared to the complexation between H and G3.

dx.doi.org/10.1021/jo400752d | J. Org. Chem. 2013, 78, 9004−9012

Interestingly, the calculated proton affinity of the respective amine of the guest molecule G2 (PA = 1178.7 kJ· mol^{-1}) was found to be very close to that of the host molecule H (SI Figure 6). This tends to suggest that there is a lesser possibility of any proton transfer from the guest molecule G2 to the host H during the complexation process or the H-bonded adduct formation. Thus, the observed small enhancement (Figure 9) in pyrene-based emission intensity is probably due to an effective C−H···N hydrogen bond formation involving hydrogen atoms of the polarized methylene groups (−CH_2−) next to the cationic ammonium center and the unshared pair of electrons of the NH_H moiety of the host molecule H. This is supported by the observed substantial complexation-induced shifts ($\Delta\delta$ = 0.47 and 0.31 ppm, respectively, for H_6 and H_7) of these methylene protons in H·G2 relative to free G2 (Figure 4). In contrast, these shifts for H_6 and H_7 for G1 in H·G1 were only 0.27 and 0.29 ppm, respectively (SI Figures 1 and 2), which indicated a relatively weaker H-bond formation.

Furthermore, appropriate orientation of protons of the NH_2^+ fragment of the respective guest molecule with respect to that of the N-atom of the NH unit in the host molecules is also expected to influence the efficiency of the proton transfer process. We have performed molecular dynamic calculations with host−guest complexes to check the frequency of closeness between the host nitrogen and guest amine hydrogens. The molecular dynamic simulations were performed for the complexes of host molecule H with guests G1 and G2 for 5 ns time period with 2 fs time steps using the Merck molecular force field (MMFF) method.[20] A total of 1000 geometries were examined to check the proton−nitrogen distance (after every 5 ps). In the case of the G1 molecule as the guest, the proton−nitrogen distances were below 2.2 Å a total of 394 times, whereas, in the case of the G2 molecule as the guest, this happened 350 times. These results again supported the possibility of more facile proton transfer from G1 to the H molecule, which is in support of the experimental observations.

CONCLUSION

In summary, we have demonstrated how appropriate design of the host and guest components helps to develop a supramolecular assembly where the threading phenomenon results in an interrupted PET and a fluorescence on response, which in turn initiates a FRET process. We have also investigated, through different spectroscopic studies, which stopper size is appropriate for the threading of the cavity of the NO_6 crown ether moiety to form a [2]pseudorotaxane complex. Detailed ^{1}H NMR spectroscopic studies revealed that the guest molecules G1, G2, and G3 are able to thread through the cavity of the host unit to form the 1:1 complex. However, for G4, which was substituted with relatively bulkier 3,5-di-*tert*-butyl groups, no complexes with the host unit were formed. The association constants for adducts H·G1, H·G2, and H·G3 evaluated from the ITC measurements showed a systematic increase in values on changing the stopper from butyl to 4-*tert*-butylphenyl in the guest molecules. The obtained thermodynamic data indicate that the complexation process is also influenced by the nature of the stopper units. That is, the complexation of H with guests G1 and G3 is exclusively driven by a large positive entropic gain and is accompanied by a small negative enthalpy change. In contrast, the complexation of H with G2 is driven by a large positive entropic gain along with a small positive change in enthalpy. The subtle difference in the nature of the stopper units of the guest molecules influencing the complexation process were also observed in the emission spectral studies. In all cases different degrees of emission enhancement due to interruption of the PET process were observed on initial addition of the guest molecules, which initiates a FRET process during complexation. Finally, the computational studies revealed that there was a possibility of proton transfer from the guest unit to the host during the complexation process, and the difference in acidity of the NH_2^+ unit of the guest molecules was mainly responsible for the different degrees of emission enhancement.

EXPERIMENTAL SECTION

Catechol, 2-[2-(2-chloroethoxy)ethoxy]ethanol, *p*-toluenesulfonyl chloride, pyren-2-ylmethanamine hydrochloride, benzylamine, 4-*tert*-butylbenzylamine, *n*-butylamine, 3,5-di-*tert*-butylbenzyl bromide, hexamethylenetetramine, and anthracene-9-carbaldehyde were obtained commercially and were used as received without any further purification. $[NH_4]PF_6$ was recrystallized from ethanolic solution before use, and all solvents were dried and distilled prior to use following standard procedures.

^{1}H NMR spectra were recorded on a 500 MHz FT NMR spectrometer at room temperature (rt). The chemical shift (δ) data and coupling constant (J) values are given in parts per million and hertz, respectively, throughout this paper unless mentioned otherwise.

Synthesis of 1. 1,2-Dihydroxybenzene (3.00 g, 27.27 mmol) was dissolved in 70 mL of freshly dried DMF in a two-neck round-bottom flask. To this solution was added K_2CO_3 powder (11.30 g, 81.81 mmol). Then the reaction mixture turned from brown to violet in color, and KI (13.60 g, 81.81 mmol) was added. This mixture was allowed to stir for 15 min, and 2-[2-(2-chloroethoxy)ethoxy]ethanol (9.10 g, 54.54 mmol) was added via a syringe at 60 °C. Then the temperature was raised to 80 °C and the mixture allowed to stir for 5 days. The solvent was removed under reduced pressure and the residue extracted three times with $CHCl_3$ and water. Organic layers were combined and dried over anhydrous sodium sulfate. Solvent was removed under reduced pressure to give a crude product which was purified on a silica gel column using methanol/dichloromethane (2:98, v/v) as the eluent to yield **1** (5.40 g, 53.3%) as a sticky brown semisolid. ^{1}H NMR (500 MHz, $CDCl_3$, δ, ppm): 3.58 (4H, t, J = 4.5), 3.66 (4H, t, J = 4.5), 3.74−3.70 (8H, m), 3.86 (4H, t, J = 4.5), 4.15 (4H, t, J = 4), 6.89 (4H, s). Anal. Calcd for $C_{18}H_{30}O_8$: C, 57.74; H, 8.08. Found: C, 57.67; H, 8.01. ESI-MS: m/z calcd for $C_{18}H_{30}O_8Na$ 397.19, found 397.41 $[M + Na]^+$.

Synthesis of 2. Compound **1** (5.40 g, 14.56 mmol) was dissolved in THF (40 mL), and 5 mL of NaOH solution (10 M) was added to it at 0 °C. *p*-Toluenesulfonyl chloride (9.70 g, 50.96 mmol) in 15 mL of THF was added dropwise over a period of 30 min to the reaction mixture at 0 °C with vigorous stirring. The reaction was stopped after 5 days. The solvent was removed under reduced pressure and the residue extracted three times with $CHCl_3$ and water. The organic layers were combined and dried over anhydrous sodium sulfate. Solvent was removed under reduced pressure to give a crude product. This was purified on a silica gel column using CH_3OH/CH_2Cl_2 (2:98, v/v) as the eluent to yield **2** (7.75 g, 78.0%) as a sticky brown mass. ^{1}H NMR (500 MHz, $CDCl_3$, δ, ppm): 2.41 (6H, s), 3.59 (4H, t, J = 4.0), 3.69−3.63 (8H, m), 3.82 (4H, t, J = 5.0), 4.13 (4H, t, J = 5.0), 6.90 (4H, s), 7.31 (4H, d, J = 8.0), 7.79 (4H, d, J = 8.5). ^{13}C NMR (δ, ppm): 150.7, 147.0, 134.8, 131.8, 129.8, 128.0, 123.4, 116.2, 72.5, 71.5, 70.5, 23.3. Anal. Calcd for $C_{32}H_{42}O_{12}S_2$: C, 56.29; H, 6.20; S, 9.39. Found: C, 56.18; H, 6.14; S, 9.31. ESI-MS: m/z calcd for $C_{32}H_{43}O_{12}S_2$ 683.21, found 683.40 $[M + H]^+$.

Synthesis of H. Compound **2** (1.00 g, 1.46 mmol) was dissolved in 5 mL of freshly distilled CH_3CN in a two-neck round-bottom flask. Pyren-2ylmethanamine hydrochloride (0.43 g, 1.60 mmol) was added followed by five drops of triethylamine to get a clear solution. To this stirred solution were added K_2CO_3 (2.20 g, 16.00 mmol), KI (0.40 mg, 2.40 mmol), and 30 mL of solvent. The reaction mixture was refluxed for 18 h. Solvent was removed under reduced pressure and the residue

dx.doi.org/10.1021/jo400752d | J. Org. Chem. 2013, 78, 9004−9012

extracted three times with $CHCl_3$. The combined organic layers were dried over anhydrous sodium sulfate. The crude product was purified by being passed through an alumina column using hexane/$CHCl_3$ (2:8, v/v) as the eluent to yield H (0.49 g, 60.0%) as a sticky brown mass. ^{1}H NMR (500 MHz, CD_2Cl_2, δ, ppm): 2.86 (4H, t, J = 5.5), 3.60−3.58 (8H, m), 3.66 (4H, t, J = 5.0), 3.81 (4H, t, J = 4.5), 4.10 (4H, t, J = 4.5), 4.34 (2H, s), 6.91 (4H, s), 7.98 (2H, d, J = 7.5), 8.04 (2H, s), 8.11 (2H, d, J = 7.5), 8.17 (2H, d, J = 7.5), 8.65 (1H, d, J = 9). ^{13}C NMR (125 MHz, $CDCl_3$, δ, ppm): 150.6, 134.8, 132.9, 132.5, 132.3, 131.5, 129.8, 129.1, 128.6, 127.4, 126.6, 126.5, 126.4, 126.0, 123.2, 116.1, 72.6, 72.2, 71.5, 71.3, 70.8, 60.0, 55.8. Anal. Calcd for $C_{35}H_{39}NO_6$: C, 73.79; H, 6.90; N, 2.46. Found: C, 73.61; H, 6.82; N, 2.39. ESI-MS: m/z calcd for $C_{35}H_{40}NO_6$ 570.28, found 570.69 $[M + H]^+$.

Synthesis of 3. 3,5-Di-*tert*-butylbenzyl bromide (0.50 g, 1.76 mmol) was dissolved in a $CHCl_3$/EtOH (12:2 v/v), solvent mixture. To this solution was added hexamethylenetetramine (0.25 g, 1.76 mmol), and the reaction mixture was refluxed for 7 h. A white precipitate appeared and was filtered through a crucible and dried. Again the white precipitate was dissolved in 20 mL of EtOH and 5 mL of concd HCl solvent mixture. Then the reaction mixture was refluxed for 10 h. A white precipitate appeared and was filtered through a crucible, dissolved in 100 mL of water, and neutralized with $NaHCO_3$. Then the mixture was extracted three times with $CHCl_3$. The organic layers were combined and dried over anhydrous sodium sulfate. Solvent was removed under reduced pressure to yield **3** (0.23 g, 60.0%) as a sticky brown solid. ^{1}H NMR (500 MHz, CD_2Cl_2, δ, ppm): 7.30 (1H, s), 7.15 (2H, s), 3.80 (2H, s), 1.31 (18H, s). Anal. Calcd for $C_{15}H_{25}N$: C, 82.13; H, 11.49; N, 6.39. Found: C, 82.07; H, 11.43; N, 6.31. ESI-MS: m/z calcd for $C_{15}H_{25}N$ 219.20, found 219.02.

Synthesis of G1. Benzylamine (0.50 g, 5.20 mmol) was added to anthracene-9-carbaldehyde (1.07 g, 5.20 mmol) dissolved in dry methanol (25 mL), and the reaction mixture was stirred vigorously at room temperature. After 24 h, the reaction mixture was cooled to 0 °C. $NaBH_4$ (0.50 g) was added portionwise to the stirred cooled reaction mixture, which was stirred for another 1 h at 0 °C. The reaction mixture was allowed to reach room temperature and stirred for a further 2 h. The solvent was removed under reduced pressure, the residue was extracted three times with $CHCl_3$ and water, and the organic layers were combined and dried over anhydrous sodium sulfate. The solvent was removed under reduced pressure to give the crude product, which was purified on silica gel with CH_3OH/$CHCl_3$ (4:96, v/v) as the eluent. The desired compound was isolated as a sticky brown solid. A solution of HCl (concentrated HCl (0.5 mL) dissolved in acetone (2 mL)) was added dropwise to the sticky solid dissolved in acetone (20 mL) and the resulting solution stirred for 2 h. A white solid was formed, which was isolated by filtration and air-dried. Finally anion exchange in water using NH_4PF_6 gave the desired PF_6^- salt of G1 with a yield of 0.92 g, 40.0%. ^{1}H NMR (500 MHz, CD_2Cl_2/CD_3CN (4:1, v/v), δ, ppm): 8.63 (1H, s), 8.12 (2H, d, J = 8.0), 8.03 (2H, d, J = 8.5), 7.61 (2H, t, J = 7.5), 7.56 (2H, t, J = 7.5), 7.51 (5H, s), 5.10 (2H, s), 4.35 (2H, s). ^{13}C NMR (125 MHz, CD_3CN, δ, ppm): 131.3, 130.8, 130.5, 130.3, 129.9, 129.5, 129.2, 127.8, 125.6, 123.1, 121.0, 52.0, 43.1. Anal. Calcd for $C_{22}H_{20}NPF_6$: C, 59.60; H, 4.55; N, 3.16. Found: C, 59.50; H, 4.51; N, 3.11. ESI-MS: m/z calcd for $C_{22}H_{20}N$ 298.16, found 298.12 $[M - PF_6^-]^+$.

Synthesis of G2. The desired PF_6^- salt of G2 was obtained by following an experimental procedure similar to that described for G1 as a brown solid (yield 0.56 g, 55.0%). ^{1}H NMR (500 MHz, $CDCl_3$/CD_3CN (4:1, v/v), δ, ppm): 8.70 (1H, s), 8.27 (2H, d, J = 9.0), 8.16 (2H, d, J = 8.0), 7.72 (2H, t, J = 7.7), 7.60 (2H, t, J = 6.5), 5.22 (2H, s), 3.21 (2H, t, J = 8.0), 1.70−1.65 (2H, m), 1.41−1.36 (2H, m), 0.96 (3H, m). ^{13}C NMR (125 MHz, CD_3CN, δ, ppm): 131.3, 130.8, 129.5, 127.6, 125.7, 123.3, 121.1, 118.1, 117.3, 48.8, 44.0, 27.4, 19.3, 12.7. Anal. Calcd for $C_{19}H_{22}NPF_6$: C, 55.75; H, 5.42; N, 3.42. Found: C, 55.68; H, 5.37; N, 3.38. ESI-MS: m/z calcd for $C_{19}H_{22}N$ 264.17, found 264.14 $[M - PF_6^-]^+$.

Synthesis of G3. 4-*tert*-Butylbenzylamine (0.25 g, 1.53 mmol) was added to anthracene-9-carbaldehyde (0.31g, 1.53 mmol) dissolved in dry methanol (25 mL), and the reaction mixture was stirred vigorously at room temperature. A white precipitate appeared after 24 h and was filtered through a crucible and dried. It was further dissolved in 5 mL of $CHCl_3$. To this mixture was added 25 mL of methanol, and the reaction mixture was cooled to 0 °C. $NaBH_4$ (0.50 g) was added portionwise to the stirred cooled reaction mixture, which was stirred for another 1 h at 0 °C. The solvent was removed under reduced pressure, the residue was extracted three times with $CHCl_3$ and water, and the organic layers were combined and dried over anhydrous sodium sulfate. The solvent was removed under reduced pressure to give the compound as a sticky brown solid. A solution of HCl (concentrated HCl (0.5 mL) dissolved in acetone (2 mL)) was added dropwise to the sticky solid dissolved in acetone (20 mL) and the resulting mixture stirred for 2 h. A white solid was formed, which was isolated by filtration and air-dried. Finally, anion exchange in water using NH_4PF_6 gave the desired PF_6^- salt of G3 with a yield of 0.45 g, 60.0%. ^{1}H NMR (500 MHz, $CDCl_3$/CD_3CN (4:1, v/v), δ, ppm): 8.65 (1H, s), 8.11 (2H, d, J = 7.5), 7.96 (2H, d, J = 8.0), 7.58−7.55 (6H, m), 7.51 (2H, m), 5.12 (2H, s), 4.37 (2H, s), 1.38 (9H, s). ^{13}C NMR (125 MHz, CD_3CN, δ, ppm): 153.4, 131.5, 131.0, 130.9, 130.5, 129.7, 127.8, 127.6, 126.3, 125.8, 123.3, 121.4, 51.7, 42.9, 34.7, 30.7. Anal. Calcd for $C_{26}H_{28}NPF_6$: C, 62.52; H, 5.65; N, 2.80. Found: C, 62.42; H, 5.60; N, 2.72. ESI-MS: m/z calcd for $C_{26}H_{28}N$ 354.22, found 354.27 $[M - PF_6^-]^+$.

Synthesis of G4. The desired PF_6^- salt of G4 was obtained by following an experimental procedure similar to that described for G3 as a white solid (yield 0.47 g, 57.0%). ^{1}H NMR (500 MHz, $CDCl_3$/CD_3CN (4:1, v/v), δ, ppm): 8.38 (1H, s), 8.20 (2H, d, J = 8.5), 7.99 (2H, d, J = 8.5), 7.48−7.42 (4H, m), 7.39 (1H, s), 7.29 (2H, s), 4.67 (2H, s), 4.05 (2H, s), 1.36 (18H, s). ^{13}C NMR (125 MHz, CD_3CN, δ, ppm): 151.1, 139.3, 135.1, 134.5, 131.7, 130.5, 129.1, 127.4, 126.2, 125.3, 124.7, 122.9, 121.4, 54.1, 44.3, 34.7, 31.0. Anal. Calcd for $C_{29}H_{35}NPF_6$: C, 64.20; H, 6.50; N, 2.58. Found: C, 64.18; H, 6.46; N, 2.56. ESI-MS: m/z calcd for $C_{30}H_{36}N$ 410.28, found 410.35 for $[M - PF_6^-]^+$.

■ ASSOCIATED CONTENT

Supporting Information

Determination of the binding constant, computational method, B3LYP/6-31G*-optimized coordinates, and some spectroscopic results. This material is available free of charge via the Internet at http://pubs.acs.org.

■ AUTHOR INFORMATION

Corresponding Authors

*E-mail: ganguly@csmcri.org.

*E-mail: a.das@ncl.res.in.

Notes

The authors declare no competing financial interest.

‖**Previous Affiliation** for M.G. and A.D.: CSIR-Central Salt and Marine Chemicals Research Institute, Bhavnagar, Gujarat 364002, India.

■ ACKNOWLEDGMENTS

A.D. thanks the Department of Science and Technology (DST), New Delhi, India, for financial support. A.D. and B.G. thank the Council of Scientific and Industrial Research (CSIR) (Network Projects M2D and MSM-CSC-0129) for support. A.K.M. and M.S. thank the CSIR (India) for Research Fellowship. We thank the anonymous reviewers for their suggestions and comments, which have helped us to improve the paper.

■ REFERENCES

(1) (a) Sutherland, I. O. *Chem. Soc. Rev.* **1986**, *15*, 63. (b) Stoddart, J. E. *Top. Stereochem.* **1988**, *17*, 205. (c) Ishow, E.; Credi, A.; Balzani, V.; Sapdola, F.; Mandolini, L. *Chem.—Eur. J.* **1999**, *5*, 984. (d) Cantrill, S.

J.; Pease, A. R.; Stoddart, J. F. *J. Chem. Soc., Dalton Trans.* **2000**, 3715. (e) Meilion, J. C.; Voyer, N.; Biron, E.; Sanschagrin, F.; Stoddart, J. F. *Angew. Chem., Int. Ed.* **2000**, *39*, 143. (f) Dichtel, W. R.; Miljanić, O. S.; Zhang, W.; Spruell, J. M.; Patel, K.; Aprahamian, I.; Heath, J. R.; Stoddart, J. F. *Acc. Chem. Res.* **2008**, *41*, 1750. (g) Niu, Z.; Gibson, H. W. *Chem. Rev.* **2009**, *109*, 6024. (h) Suresh, M.; Mandal, A. K.; Suresh, E.; Das, A. *Chem. Sci.* **2013**, *4*, 2380. (i) Späth, A.; König, B. *Beilstein J. Org. Chem.* **2010**, *6*, 32.

(2) (a) Bossi, M.; Belov, V.; Polyakova, S.; Hell, W. S. *Angew. Chem., Int. Ed.* **2006**, *45*, 7462. (b) Yen, M. L.; Li, W. S.; Lai, C. C.; Chao, I.; Chiu, S. H. *Org. Lett.* **2006**, *8*, 3223. (c) Cooke, G.; Woisel, P.; Bria, M.; Delattre, F.; Garety, J. F.; Hewage, S. G.; Robani, G.; Rosair, G. M. *Org. Lett.* **2006**, *8*, 1423. (d) Olson, A. M.; Braunschweig, A. B.; Fang, L.; Ikeda, T.; Klajn, M. R.; Trabolsi, A.; Wesson, J. P.; Benilez, D.; Mirkin, C. A.; Grzybowski, B. A.; Stodart, J. F. *Angew. Chem., Int. Ed.* **2009**, *48*, 1. (e) Lohmann, F.; Ackermann, D.; Famulok, M. *J. Am. Chem. Soc.* **2012**, *134*, 11884.

(3) (a) Kelly, T. R. *Acc. Chem. Res.* **2001**, *34*, 514. (b) Schalley, C. A.; Beizai, K.; Vögtle, F. *Acc. Chem. Res.* **2001**, *34*, 465. (c) Makita, Y.; Kihara, N.; Takata, T. *J. Org. Chem.* **2008**, *73*, 9245.

(4) (a) Barrell, M. J.; Leigh, D. A.; Lusby, P. J.; Slawin, A. M. Z. *Angew. Chem., Int. Ed.* **2008**, *47*, 8036. (b) Yang, C. H.; Prabhakar, C.; Huang, S. L.; Lin, Y. C.; Tan, W. S.; Misra, N. C.; Sun, W. T.; Yang, J. S. *Org. Lett.* **2011**, *13*, 5632. (c) Dial, B. E.; Pellechia, P. J.; Smith, M. D.; Shimizu, K. D. *J. Am. Chem. Soc.* **2012**, *134*, 3675.

(5) (a) Keaveney, C. M.; Leigh, D. A. *Angew. Chem., Int. Ed.* **2004**, *43*, 1222. (b) Saha, S.; Flood, A. H.; Stoddart, J. F.; Impellizzeni, S.; Silvi, S.; Venturi, M.; Credi, A. *J. Am. Chem. Soc.* **2007**, *129*, 12159. (c) Yamauchi, A.; Miyawaki, A.; Takashima, Y.; Yamaguchi, H.; Harada, A. *J. Org. Chem.* **2010**, *75*, 1040. (d) Fahrenbach, A. C.; Bruns, C. J.; Cao, D.; Stoddart, J. F. *Acc. Chem. Res.* **2012**, *45*, 1581. (e) Zhang, Z. J.; Han, M.; Zhang, H. Y.; Liu, Y. *Org. Lett.* **2013**, *15*, 1698.

(6) (a) Okamoto, A.; Tanaka, K.; Saito, I. *J. Am. Chem. Soc.* **2004**, *126*, 9458. (b) van Noort, D.; Landweber, L. F. *Nat. Comput.* **2005**, *4*, 163. (c) Romuald, C.; Busseron, E.; Coutrot, F. *J. Org. Chem.* **2010**, *75*, 6516. (d) Horie, M.; Suzaki, Y.; Hashizume, D.; Abe, T.; Wu, T.; Sassa, T.; Hosokai, T.; Osakada, K. *J. Am. Chem. Soc.* **2012**, *134*, 17932. (e) Suresh, M.; Mandal, A. K.; Kesharwani, M. K.; Adarsh, N. N.; Ganguly, B.; Kanaparthi, R. K.; Samanta, A.; Das, A. *J. Org. Chem.* **2011**, *76*, 138. (f) Mandal, A. K.; Suresh, M.; Das, P.; Das, A. *Chem.—Eur. J.* **2012**, *18*, 3906. (g) Mandal, A. K.; Suresh, M.; Das, A. *Org. Biomol. Chem.* **2011**, *9*, 4811.

(7) (a) Balllardini, R.; Balzani, V.; Leon, M. C.; Credi, A.; Gandolfi, M. T.; Ishow, E.; Perkins, J.; Stoddart, J. F.; Tseng, H. R.; Wenger, S. *J. Am. Chem. Soc.* **2002**, *124*, 12786. (b) Leong, W. L.; Vittal, J. J. *Chem. Rev.* **2011**, *111*, 688.

(8) (a) Kolchinski, A. G.; Busch, D. H.; Alcock, N. W. *Chem. Commun.* **1995**, 1289. (b) Jones, J. W.; Gibson, H. W. *J. Am. Chem. Soc.* **2003**, *125*, 7001.

(9) (a) deSilva, A. P.; Gunaratne, H. Q. N.; McCoy, C. P. *Nature* **1993**, *364*, 42. (b) deSilva, A. P.; Gunaratne, H. Q. N.; Gunnlaugsson, T.; Huxley, A. J. M.; MeCoy, C. P.; Rademacher, J. T.; Rice, T. E. *Chem. Rev.* **1997**, *97*, 1515. (c) Ghosh, P.; Bharadwaj, P. K.; Roy, J.; Ghosh, S. *J. Am. Chem. Soc.* **1997**, *119*, 11903. (d) Chen, X.; Pradhan, T.; Wang, F.; Kim, J. S.; Yoon, J. *Chem. Rev.* **2012**, *112*, 1910. (e) Bull, S. D.; Davidson, M. G.; van den Elsen, J. M. H.; Fossey, J. S.; Jenkins, A. T. A.; Jiang, Y.; Kubo, Y.; Marken, F.; Sakurai, K.; Zhao, J.; James, T. D. *Acc. Chem. Res.* **2013**, *46*, 312.

(10) (a) Cantrill, S. J.; Fulton, D. A.; Heiss, A. M.; Pease, A. R.; Stoddart, J. F.; White, A. J. P.; Williams, D. J. *Chem.—Eur. J.* **2000**, *6*, 2274. (b) Zhang, C.; Li, S.; Zhang, J.; Zhu, K.; Li, N.; Huang, F. *Org. Lett.* **2007**, *9*, 5553. (c) Jiang, W.; Winkler, H. D. F.; Schalley, C. A. *J. Am. Chem. Soc.* **2008**, *130*, 13852. (d) Turnbull, W. B.; Daranas, A. H. *J. Am. Chem. Soc.* **2003**, *125*, 14859.

(11) (a) Wiseman, T.; Williston, S.; Brandts, J. F.; Lin, L.-N. *Anal. Biochem.* **1989**, *179*, 131. (b) Kaufmann, L.; Dzyuba, E. V.; Malberg, F.; Löw, N. L.; Groschke, M.; Brusilowskij, B.; Huuskonen, J.; Rissanen, K.; Kirchner, B.; Schalley, C. A. *Org. Biomol. Chem.* **2012**, *10*, 5954.

(12) (a) Ashton, P. R.; Chrystal, E. J. T.; Glink, P.; Menzer, S.; Schiavo, C.; Spencer, N.; Stoddart, J. F.; Tasker, P. A.; White, A. J. P.; Williams, D. J. *Chem.—Eur. J.* **1996**, *2*, 709.

(13) (a) Jiang, W.; Winkler, H. D. F.; Schalley, C. A. *J. Am. Chem. Soc.* **2008**, *130*, 13852.

(14) (a) Bonal, C.; Israëli, Y.; Morel, J. P.; Morel-Desrosiers, N. *J. Chem. Soc., Perkin Trans.* **2001**, *2*, 1075. (b) Liu, Y.; Guo, D. S.; Zhang, H. Y.; Ma, Y. H.; Yang, E. C. *J. Phys. Chem. B* **2006**, *110*, 3428. (c) Liu, Y.; Ma, Y. H.; Chen, Y.; Guo, D. S.; Li, Q. *J. Org. Chem.* **2006**, *71*, 6468. (d) Chen, L.; Zhang, Y. M.; Liu, Y. *J. Phys. Chem. B* **2012**, *116*, 9500. (e) Chen, L.; Zhang, H. Y.; Liu, Y. *J. Org. Chem.* **2012**, *77*, 9766.

(15) (a) Lakowicz, J. R. *Principles of Fluorescence Sspectroscopy*, 3rd ed.; Springer: New York, 2006.

(16) (a) Mandal, A. K.; Suresh, M.; Das, P.; Das, A. *Chem.—Eur. J.* **2012**, *18*, 3906.

(17) (a) Watrob, H. M.; Pan, C. P.; Barkley, M. D. *J. Am. Chem. Soc.* **2003**, *125*, 7336.

(18) (a) Lee, C.; Yang, W.; Parr, R. G. *Phys. Rev. B* **1988**, *37*, 785. (b) Hehre, W. J.; Radom, L.; Schleyer, P. V. R.; Pople, J. A. *Ab Initio Molecular Orbital Theory*; Wiley: New York, 1988. (c) Becke, A. D. *J. Chem. Phys.* **1993**, *98*, 5648.

(19) (a) Cancès, E.; Mennucci, B.; Tomasi, J. *J. Chem. Phys.* **1997**, *107*, 3032. (b) Mennucci, B.; Tomasi, J. *J. Chem. Phys.* **1997**, *106*, 5151. (c) Barone, V.; Cossi, M.; Tomasi, J. *J. Chem. Phys.* **1997**, *107*, 3210. (d) Barone, V.; Cossi, M.; Tomasi, J. *J. Comput. Chem.* **1998**, *19*, 404. (e) Tomasi, J.; Mennucci, B.; Cancès, E. *J. Mol. Struct.* **1999**, *464*, 211.

(20) (a) Halgren, T. *J. Comput. Chem.* **1996**, *17*, 490. (b) Halgren, T. *J. Comput. Chem.* **1996**, *17*, 520. (c) Halgren, T. *J. Comput. Chem.* **1996**, *17*, 553.